

# Large Arctic Temperature Change at the Wisconsin-Holocene Glacial Transition

Kurt M. Cuffey,\* Gary D. Clow, Richard B. Alley, Minze Stuiver, Edwin D. Waddington, Richard W. Saltus

Analysis of borehole temperature and Greenland Ice Sheet Project II ice-core isotopic composition reveals that the warming from average glacial conditions to the Holocene in central Greenland was large, approximately 15°C. This is at least three times the coincident temperature change in the tropics and mid-latitudes. The coldest periods of the last glacial were probably 21°C colder than at present over the Greenland ice sheet.

The Greenland Ice Sheet Project II (GISP2) deep ice core has yielded a remarkable history of the oxygen isotopic composition of central Greenland snowfall [ $\delta^{18}\text{O}$  of ice (1)] that extends through the last glacial period (2). The nearby Greenland Ice Core Project (GRIP) record (3) is essentially identical for ice formed after the 110,000-year-old Eemian interglacial, and both are similar to isotope histories obtained in other Greenland cores, giving confidence that these cores record aspects of regional climate (4). Using both empirical data (5) and physical models for isotope fractionation (6), paleoclimatologists have interpreted  $\delta^{18}\text{O}$  to be a measure of environmental temperature  $T$  at the core site, through a simple relation that we call the isotopic paleothermometer:  $\delta^{18}\text{O} = \alpha T + \beta$ , where  $\alpha$  and  $\beta$  are constants. There are two obstacles to making this interpretation sound. First, the coefficients  $\alpha$  and  $\beta$  are not known a priori (7–9) because many factors in addition to local environmental temperature affect isotopic composition. These include changes in sea-surface composition and temperature (10), changes in atmospheric circulation (11), changes in cloud temperature, which may be different from changes in surface temperature (12), changes in the seasonality of precipitation (13), and postdepositional isotopic exchange in the snowpack (14). Second, all of these factors may vary through time in such a way that a single, linear relation between  $\delta^{18}\text{O}$  and  $T$  is inappropriate. Thus, there is

strong motivation to seek paleotemperature information that is entirely independent of isotopic history (15, 16) to calibrate the paleothermometer. We have obtained such information by measuring temperature at depth in the ice sheet, and we use this information to evaluate  $\alpha$  and  $\beta$ .

During the summer of 1994, one of us (G.D.C.) measured temperature in the 3044-m-deep GISP2 core hole from 70 m below the surface to the base of the ice sheet. At that time, the thermal perturbation from drilling had decayed to less than 0.04°C, so the temperature in the borehole matched the temperature in the surrounding ice sheet at this accuracy and better (17). To determine the coefficients  $\alpha$  and  $\beta$  in the isotopic paleothermometer, we used the GISP2  $\delta^{18}\text{O}$  record and an initial guess for  $\alpha$  and  $\beta$  to specify a 100,000-year history of environmental temperature. We then calculated subsurface temperatures using  $T$  as the forcing function on the upper surface of the ice sheet in a linked heat- and ice-flow model. Finally, we adjusted  $\alpha$ ,  $\beta$ , and the geothermal heat flux from the underlying bedrock, using the Levenberg-Marquardt method (18) to minimize the mismatch between modeled and measured subsurface temperatures. For this purpose we defined the mismatch index  $J$  as a weighted integral over ice depth  $z$  of the squared difference between modeled and measured subsurface temperatures ( $M$  and  $\Theta$ , respectively)

$$J \equiv \int \frac{[M(z) - \Theta(z)]^2}{[\sigma_t^2(z) + f\sigma_D^2(z)]} dz \quad (1)$$

Here  $\sigma_D$  and  $\sigma_t$  are weighting functions that assign relative importance to misfit in various parts of the borehole:  $\sigma_D$  assigns more weight to the upper part of the borehole, where the temperature does not depend on poorly known ice dynamical quantities, and  $\sigma_t$  assigns more weight to the lower part of the borehole, where the temperature depends on longer intervals of the surface temperature history. The parameter  $f$ , which is adjustable, controls the trade-off between these opposing weighting schemes

(19). The solution that minimizes  $J$  is non-unique because we are free to choose  $f$ .

The heat-flow component of our model is a numerical solution to the advection-diffusion equation with heat sources (20). The model is one-dimensional (vertical), with a movable upper boundary to allow changes in the ice sheet thickness. These changes, and the vertical ice velocity responsible for heat advection, are calculated with standard glaciologic assumptions for flow on the flank of an ice divide with simple parameterizations to account for two-dimensional effects. In our model, the ice sheet responds to local changes in snow accumulation rate, surface temperature, and ice crystal fabric and to distant changes in ice margin position (21). To calculate vertical heat advection most confidently, and to account for two-dimensional effects on ice particle paths, we tuned the vertical velocity so that the modern depth-age scale matched our model within a small tolerance. Because of this tuning, our conclusions are insensitive to poorly known aspects of the ice dynamics. The GISP2 depth-age scale was determined by annual layer counts to about 40,000 years ago (40 ka) and by correlation to the ocean-core time scale (SPECMAP) through analysis of the oxygen isotopic composition of  $\text{O}_2$  gas for older ice (22–24).

The snow accumulation rate history  $b(t)$  exerts a dominant control on ice sheet thickness and vertical ice flow, and hence vertical heat advection. For the most recent 35,000 years, we derived  $b(t)$  from the layer thickness measurements of Meese and others (23), corrected for ice-flow thinning. Our correction uses strain calculations as done previously (24, 25), but we also included the dependence of layer thinning on the thickness history of the ice sheet (26, 27), which in turn depends on the temperature history. Before 35 ka in the model

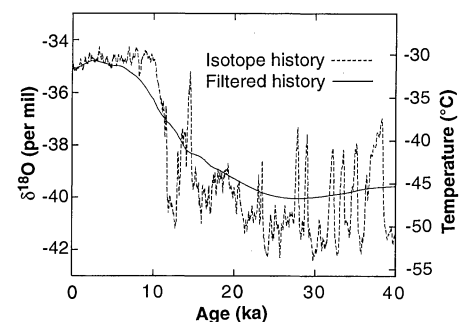


**Fig. 1.** The central Greenland  $\delta^{18}\text{O}$  history for the most recent 40,000 years. The smooth curve results when this history is filtered to mimic the thermal averaging in the ice sheet (45). All temperature histories that give this same curve when filtered are indistinguishable to borehole thermometry (29). The right axis shows our calibrated temperature scale.

K. M. Cuffey, Department of Geological Sciences, Box 351310, University of Washington, Seattle, WA 98195, USA.

G. D. Clow, U.S. Geological Survey, Mail Stop 975, Menlo Park, CA 94025, USA.

R. B. Alley, Earth System Science Center and Department of Geosciences, The Pennsylvania State University, University Park, PA 16802, USA.

M. Stuiver, Quaternary Isotope Laboratory and Department of Geosciences, Box 351310, University of Washington, Seattle, WA 98195, USA.

E. D. Waddington, Geophysics Program, Box 351650, University of Washington, Seattle, WA 98195, USA.

R. W. Saltus, U.S. Geological Survey, Mail Stop 964, Denver Federal Center, Denver, CO 80225, USA.

\*To whom correspondence should be addressed.

runs, we calculate  $b(t)$  from the oxygen isotopes using a linear correlation between  $\delta^{18}\text{O}$  and our  $b(t)$  for the most recent 35,000 years (28).

Because heat diffusion damps high-frequency temperature changes as they propagate from the surface down into the ice sheet (thermal averaging), information on rapid environmental temperature changes in the past is poorly retained by the present-day temperature field  $\Theta(z)$  in the ice sheet (29). Thermal averaging is more extensive for older climatic events. In contrast, the GISP2  $\delta^{18}\text{O}$  record retains information about rapid climatic changes. If we degrade the  $\delta^{18}\text{O}$  record so that it retains only the age-dependent low-frequency content that can be recovered from the present-day temperature field (Fig. 1), then the abrupt termination of the Younger Dryas, the Younger Dryas itself, and the Bølling/Allerød period become minor features of the history, and earlier interstadial events are no longer

evident. Thus, our isotope calibration is sensitive mainly to the long warming from full glacial conditions to the Holocene, and to Holocene temperature changes (30).

We find the optimal linear paleothermometer to be  $\delta^{18}\text{O} = 0.327T - 24.8$  if we assume ice dynamics are well known ( $f = 1$ ; refer to Eq. 1), and  $\delta^{18}\text{O} = 0.335T - 24.5$  if we assume ice dynamics are poorly known ( $f = 1000$ ) (31). Using these calibration constants, we find a remarkably good fit between the temperatures measured in the borehole (Fig. 2) and the corresponding modeled temperatures; the model accounts for 99.88% of the variance of the measured profile relative to steady-state. This is strong evidence that  $\delta^{18}\text{O}$  is indeed a faithful proxy for long-term average temperature at this site. There is no better explanation for the success of such a simple calibration, given the small number of free parameters in the inversion.

However, the fit is not perfect. For in-

stance, the isotope record underpredicts the magnitude of cooling in the late Holocene. If we allow some time variation of  $\alpha$  (32),  $J$  is minimized with  $\alpha \approx 0.33$  per mil  $^{\circ}\text{C}^{-1}$  (33) during the deglacial transition. For much of the Holocene the optimal value for  $\alpha$  is 0.25 per mil  $^{\circ}\text{C}^{-1}$ . In the most recent several centuries, for which higher frequency climate changes are resolved by the borehole temperatures,  $\alpha$  becomes larger (0.46 per mil  $^{\circ}\text{C}^{-1}$ ) and closer to the value inferred from modern temperature records (33). Our result shows that the general circulation model of Jouzel *et al.* (8) can provide better estimates of past values of  $\alpha$  than the value of 0.60 to 0.67 per mil  $^{\circ}\text{C}^{-1}$  derived from the modern spatial correlation; they predict  $\alpha \approx 0.43$  per mil  $^{\circ}\text{C}^{-1}$  for the deglacial transition by linking changes in atmospheric circulation and source temperature to a physical model of isotope fractionation (34).

The low value of  $\alpha$  that we find for the deglacial transition is well-constrained (Fig. 3) and insensitive to changes in ice dynamical parameters (Table 1). The average temperature difference between the Wisconsin Glaciation and the Holocene is therefore large (Fig. 1),  $14^{\circ}$  to  $16^{\circ}\text{C}$ , and the coldest periods of the last glacial were probably  $21^{\circ}\text{C}$  colder than at present (Fig. 1). The climatic deglacial temperature change (at constant elevation) may be  $1^{\circ}$  to  $2^{\circ}\text{C}$  larger than this because the Greenland ice sheet was probably thinner during the glacial as a result of a substantial reduction in accumulation rate. Geologic evidence suggests that the margins of the ice sheet retracted by about 100 km during the Wisconsin-Holocene transition (35). Using this value, and assuming a symmetrical retreat of east and west margins, we estimate that the ice sheet thickened by 250 m from the last glacial maximum to the present, and at least 100 m from average glacial conditions to the present (36).

**Table 1.** Sensitivity of  $\alpha = d(\delta^{18}\text{O})/dT$  to changes in ice dynamical quantities that are poorly known or uncertain (47). The constant  $\alpha$  is most sensitive to adjustments of the age-depth relation (the time scale); however, even this sensitivity is minor. The 2% uncertainty in age at the Younger Dryas termination (1680 m in depth) is an estimate by Alley *et al.* (24).

Model adjustment	$\alpha$ (per mil $^{\circ}\text{C}^{-1}$ )	$\Delta T$ ( $^{\circ}\text{C}$ )	
		Average glacial to Holocene	Coldest glacial to Holocene
No marginal retreat	0.327	15.3	21.4
Initial temperature $4^{\circ}\text{C}$ warmer	0.328	15.2	21.3
Initial temperature $4^{\circ}\text{C}$ colder	0.328	15.2	21.3
No north-south spreading	0.328	15.2	21.3
Use uncorrected $b(t)$	0.328	15.2	21.3
No fabric evolution	0.327	15.3	21.4
Age reduced by 2% at 1680 m and by 20% at 2800-m depth	0.341	14.7	20.5
Age increased by 2% at 1680 m and by 20% at 2800-m depth	0.313	16.0	22.4

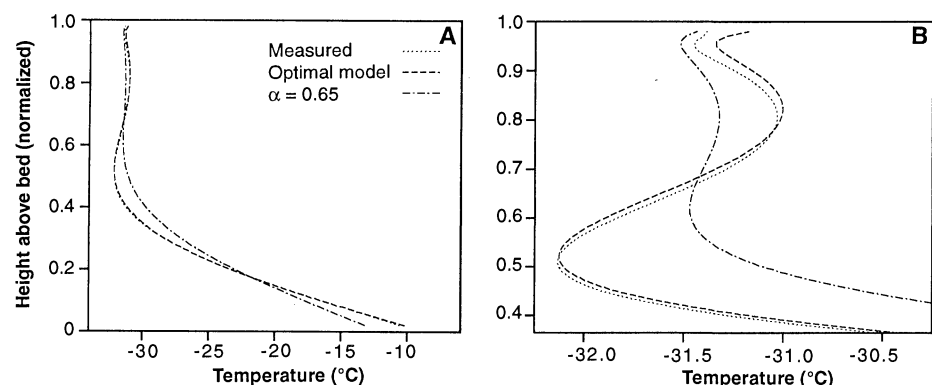


**Fig. 2.** Comparison of measured and modeled temperatures within the ice sheet, as functions of height above the ice sheet bed (normalized to the thickness of the ice sheet). (A) The full ice sheet thickness. At this scale, the measurements and the optimal model results are indistinguishable. (B) The upper part of the ice sheet. The Little Ice Age, the mid-Holocene warmth, and the cold glacial are immediately evident in the temperature profile, as they are in the GRIP hole (46). The temperature increases considerably toward the bed because of geothermal heating. The best possible fit with the approximate modern spatial value of  $\alpha = 0.65$  per mil  $^{\circ}\text{C}^{-1}$  (5) is a poor match to the data.

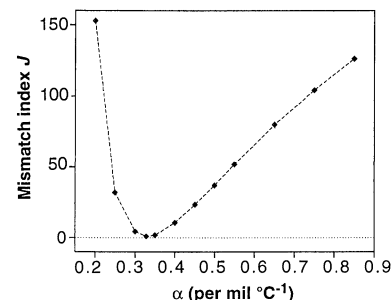


**Fig. 3.** The mismatch  $J$  between modeled and measured borehole temperature profiles, normalized to its minimum value, as a function of  $\alpha$ . The well-defined minimum shows the location of the optimal value for  $\alpha$ , 0.327 per mil  $^{\circ}\text{C}^{-1}$ . To produce this curve, we chose values for  $\alpha$ , then inverted for  $\beta$  and the geothermal flux to optimize the fit.

Recent estimates of the Wisconsin-to-Holocene warming in the low mid-latitudes are 4° to 6°C. This result is based on a variety of methods, including snow line depression studies (37), palynology (38), noble gas paleothermometry applied to ground water (39), and stable-isotope paleothermometry applied to coral reefs (40, 41). The ~8°C temperature change commonly inferred from ice-core isotopic records (37), including those from the new GISP2 and GRIP cores (2, 4), using the modern spatial value for  $\alpha$  of 0.60 to 0.67 per mil °C<sup>-1</sup>, is only slightly larger than recent estimates from the tropics. By contrast, we have shown that the temperature change in central Greenland was three to four times larger than that in the tropics, a result that is consistent with borehole temperature analyses at Dye 3 in southern Greenland (42). Many models have suggested that initially minor changes in global temperature will be magnified in the Arctic, with possibly major consequences for sea level and planetary albedo (43). Our data not only confirm that such amplification happened in the past but also show this amplification to be larger than generally thought.

## REFERENCES AND NOTES

- The value of  $\delta^{18}\text{O}$  in units of per mil is defined as  $\delta^{18}\text{O} = 1000[(R_{\text{sample}} - R_{\text{standard}})/R_{\text{standard}}]$ , where the ratio  $R \equiv [^{18}\text{O}]/[^{16}\text{O}]$  (brackets denote concentration), and the standard  $R$  is that for mean ocean water.
- P. M. Grootes *et al.*, *Nature* **366**, 552 (1993).
- W. Dansgaard *et al.*, *ibid.* **364**, 218 (1993).
- S. J. Johnsen *et al.*, *ibid.* **359**, 311 (1992).
- S. J. Johnsen, W. Dansgaard, J. W. C. White, *Tellus B* **41**, 452 (1989).
- J. Jouzel and L. Merlivat, *J. Geophys. Res. D* **89**, 11749 (1984).
- K. M. Cuffey, R. B. Alley, P. M. Grootes, J. Bolzan, S. Anandakrishnan, *J. Glaciol.* **40**, 341 (1994).
- J. Jouzel, R. Koster, R. Suozzo, G. Russell, *J. Geophys. Res. D* **99**, 25791 (1994).
- The parameters  $\alpha$  and  $\beta$  are usually derived from linear correlation of mean annual temperature and isotopic ratio with data from different sample sites across the surface of an ice sheet. The assumption that this modern spatial relationship is the same as the temporal relationship at a single site is known to be incorrect in some cases; see, for example, D. A. Peel, R. Mulvaney, B. M. Davison, *Ann. Glaciol.* **10**, 130 (1988).
- R. G. Fairbanks, *Nature* **342**, 637 (1989).
- C. D. Charles, D. Rind, J. Jouzel, R. D. Koster, R. G. Fairbanks, *Science* **263**, 508 (1994).
- G. Robin, in *The Climatic Record in Polar Ice Sheets*, G. Robin, Ed. (Cambridge Univ. Press, Cambridge, 1983), pp. 180–189.
- D. A. Fisher *et al.*, *Nature* **301**, 205 (1983); E. J. Steig, P. M. Grootes, M. Stuiver, *Science* **266**, 1885 (1994).
- I. Friedman, C. Benson, J. Gleason, in *Stable Isotope Geochemistry: A Tribute to Samuel Epstein*, J. O'Neil and I. R. Kaplan, Eds. (Spec. Publ. 3, Geochemical Society, San Antonio, TX, 1991), pp. 211–221; R. A. Sommerfeld, C. Judy, I. Friedman, *ibid.*, pp. 205–210.
- S. J. Johnsen, in *Isotopes and Impurities in Snow and Ice: Proceedings of the Grenoble Symposium* (International Association of Hydrological Sciences, Publ. 118, Bartholomew, Dorking-Surrey, UK), pp. 388–392. W. S. B. Paterson and G. K. C. Clarke, *Geophys. J. R. Astron. Soc.* **55**, 615 (1978).
- D. Dahl-Jensen and S. J. Johnsen, *Nature* **320**, 250 (1986).
- Temperatures were measured in the fluid-filled section of the borehole with an updated version of the system described in G. D. Clow *et al.*, *U.S. Geol. Surv. Open-File Rep.* 95-490 (1995). Under the environmental conditions at GISP2, the system sensitivity is 0.00014°C; the accuracy of the measurements traced to the National Institute of Standards and Technology is ~0.0045°C. Temperature measurements were acquired every 2 s while lowering a custom sensor with 20 thermistor beads down the hole at ~6 cm s<sup>-1</sup>. Instrumental noise during this experiment was limited to less than 0.001°C. Data from the moving sensor were then deconvolved to find the stationary borehole temperatures by the methods described in R. W. Saltus and G. D. Clow, *U.S. Geol. Surv. Open-File Rep.* 94-254 (1994). The precision of the completely processed data is estimated to be better than 0.001°C for wavelengths greater than about 6 m. Drilling activities between 1990 and 1993 disturbed the temperatures in the ice surrounding the borehole. Comparison of temperature measurements acquired in 1994 and 1995 in the deep borehole, and temperatures acquired to 163 m in a nearby air-filled hole, shows that the magnitude of the disturbance in 1994 was about 0.04°C near the top of the fluid-filled section of the main borehole. This disturbance diminished to about 0.001° to 0.002°C at 400 m in depth and remained at this level to the bottom of the hole. Because the disturbance is largely restricted to the upper part of the borehole, its effect on our inferred deglacial temperature change is negligible (about 1.5% of the temperature change).
- W. H. Press, S. A. Teukolsky, W. T. Vetterling, B. P. Flannery, *Numerical Recipes in C* (Cambridge Univ. Press, Cambridge, ed. 2, 1992), pp. 683–685.
- Poorly known ice dynamical quantities such as ice rheology, ancient snowfall rates, ice sheet geometry changes, and initial temperature constitute the major sources of uncertainty in calculating subsurface temperatures. This uncertainty is large deep in the borehole and small near the surface, suggesting that we should ascribe more importance to misfit in the upper part of the borehole:  $\sigma_D$  is a rigorous means of doing so. However, temperatures high in the borehole depend on only the most recent several centuries of the temperature history, whereas temperatures deep in the ice sheet depend on many tens of thousands of years of the temperature history. This suggests we should ascribe more importance to misfit in the lower part of the borehole, to find the isotopic paleothermometer that applies best to the whole isotopic history:  $\sigma_I$  is a rigorous means of doing so. We do not know what the most appropriate balance between these opposing weighting schemes should be; therefore, we introduce the trade-off parameter  $f$  and show that our result does not depend significantly on the choice of weighting scheme.
- S. V. Patankar, *Numerical Heat Transfer and Fluid Flow* (Hemisphere, Washington, DC, 1980).
- The model has 130 to 150 control volumes in the ice sheet (depending on the thickness history) and extends 10 km into bedrock. The model was tested against analytical solutions for sinusoidal surface-temperature forcing and uniform ice velocity, with the time step chosen to give 0.001°C accuracy. The vertical velocity at a given level in the ice sheet equals the ice flux divergence beneath that level. The thickness changes at a rate equal to the imbalance between snowfall and flux divergence of the entire thickness. Changes in slope and slope gradient of the ice sheet are calculated by assuming that the ice sheet evolves through a series of steady-state geometries, except in the response to marginal forcing. For the latter, the ice sheet responds as a diffusive system in a manner that is consistent with the full two-dimensional model of R. B. Alley and I. M. Whilans [*J. Geophys. Res.* **C 89**, 6487 (1984)]. At GISP2 it is not necessary to consider horizontal heat advection because the elevation difference between GISP2 and the ice divide is small. The position of the ice divide has probably changed through time [S. Anandakrishnan, R. B. Alley, E. D. Waddington, *Geophys. Res. Lett.* **21**, 441 (1994)]. As long as GISP2 has remained more than several ice thicknesses from the divide, the horizontal temperature gradient at depth has not been important [W. S. B. Paterson and E. D. Waddington, *Cold. Reg. Sci. Tech.* **12**, 99 (1986)].
- The upper part of the ice core is dated by counting of annual layers (visible stratigraphy, particle counts, electrical conductivity, and oxygen isotope counts, 2, 23, 24); M. Ram and M. Illing, *J. Glaciol.* **40**, 504 (1994); K. C. Taylor *et al.*, *Nature* **366**, 549 (1993). For the lower part of the core, see M. Bender *et al.*, *ibid.* **372**, 663 (1994).
- D. A. Meese *et al.*, *Science* **266**, 1680 (1994).
- R. B. Alley *et al.*, *Nature* **362**, 527 (1993).
- C. Schott, E. D. Waddington, C. F. Raymond, *J. Glaciol.* **38**, 162 (1992).
- See, for instance, J. F. Bolzan, E. D. Waddington, R. B. Alley, D. A. Meese, *Ann. Glaciol.* **21**, 33 (1995).
- N. Cutler *et al.*, *ibid.*, p. 26.
- The snow accumulation rate in meters per year is  $b = 1.22 + 0.028\delta^{18}\text{O}$ , for  $\delta^{18}\text{O}$  in per mil.
- G. D. Clow, *Palaeogeogr. Palaeoclimatol. Palaeoecol.* **98**, 81 (1992).
- If borehole temperature measurements are sufficiently accurate, even short or ancient features of the temperature history can be detected (29, 44). However, their contribution to the modern temperature signal is negligible, so they do not affect our isotopic thermometer calibration.
- Setting high  $f$  means we do not try to match the measured temperatures deep in the borehole. By contrast, in the sensitivity tests presented later (Table 1), we do seek a match at all depths and examine how our result depends on specific inputs.
- On the basis of thermodynamics arguments and a changing relation over time between  $\delta^{18}\text{O}$  (2) and snow accumulation rates (23) from the GISP2 ice core, M. Stuiver, P. M. Grootes, and T. F. Braziunas [*Quat. Res.*, in press] inferred that  $\alpha$  had changed in response to climate changes, with smaller values during the deglacial transition.
- We find six parameters—that is  $\beta$ , the geothermal flux, and values for  $\alpha$  in each of four time intervals—that minimize  $J$  (with  $f = 100$ ) using the Levenberg-Marquardt method. We find  $\alpha$  to be 0.33 per mil °C<sup>-1</sup> before 8 ka, 0.25 per mil °C<sup>-1</sup> for the early Holocene, 0.25 per mil °C<sup>-1</sup> for the late Holocene cooling, and 0.46 per mil °C<sup>-1</sup> for the Little Ice Age to the present. We invert for only one value of  $\beta$  because the others are chosen to ensure continuity of the temperature history. Two independent studies [(7) and C. A. Shuman *et al.*, *J. Geophys. Res. D* **100**, 9165 (1995)] also found relatively high values of  $\alpha$  for recent times. This trend in  $\alpha$  could reflect a changing climate system (32); it could also indicate that  $\delta^{18}\text{O}$  is more sensitive to temperature changes over years to centuries than to temperature changes over periods of millennia or longer. The Cuffey *et al.* (7)  $\alpha$  value is slightly higher than ours (0.53 versus 0.46 per mil °C<sup>-1</sup>) because their measurements extend 40 m closer to the ice sheet surface and hence are weighted more heavily to recent temperature changes [see figure 3 in (7)].
- Changes in seasonality of snow accumulation may contribute to the difference between the spatial and temporal gradients [(7) and P. J. Fawcett, A. M. Agustsdottir, R. B. Alley, *Eos* **76** (spring suppl.), 177 (1995)]. We used raw isotopic data from the ice core, with no adjustment for changes in source-water isotopic composition, whereas Jouzel *et al.* (8) assumed that source-water changes equaled the effect of ice-volume changes on mean oceanic composition, but removed these source-effects from their calculated last glacial maximum  $\delta^{18}\text{O}$  when they estimated the spatial gradient  $\alpha$ . Recalculation of the Jouzel *et al.* (8) temporal gradient with the snowfall isotopic change uncorrected for source effects would yield an even closer match to our result.
- S. Funder and H. C. Larsen, in *Quaternary Geology of Canada and Greenland*, R. J. Fulton, Ed. (Canadian Government Publ., Ottawa, 1989), pp. 741–792.
- Three-dimensional Greenland ice sheet models also show a thickening from glacial to Holocene [A. Letreguilly, N. Reeh, P. Huybrechts, *Palaeogeogr. Palaeoclimatol. Palaeoecol. (Global Planet. Change)* **90**, 385 (1991)]. The calculated thickness histories

from all extant models have large uncertainties because changes in ice marginal position, accumulation rate, and effective ice softness are poorly known. Our thickness history is consistent with the detailed layer thickness analysis of Bolzan *et al.* (26). However, we cannot be confident that this thickness increase implies a greater climatic temperature change, because the difference between cloud and surface temperatures also may have changed.

37. W. S. Broecker and G. H. Denton, *Geochim. Cosmochim. Acta* **53**, 2465 (1989).

38. Fossil and other data are reviewed by region in H. E. Wright *et al.*, Eds., *Global Climates since the Last Glacial Maximum* (Univ. of Minnesota Press, Minneapolis, 1993).

39. M. Stute *et al.*, *Science* **269**, 379 (1995).

40. J. W. Beck *et al.*, *ibid.* **257**, 644 (1992); T. P. Guilderson, R. G. Fairbanks, J. L. Rubenstone, *ibid.* **263**, 663 (1994).

41. Estimates of the tropical glacial-Holocene warming based on planktonic microfossil assemblages are

considerably smaller [CLIMAP Project Members, *Geol. Soc. Am. Map Chart Ser. MC-36* (1981); (40)]. This discrepancy is not resolved, but a wider variety of evidence indicates  $\sim 5^{\circ}\text{C}$  of warming.

42. Interpretation of borehole temperature data from Dye 3 must include strong horizontal heat advection, which has probably changed through time, and larger uncertainties in the accumulation history compared to GISP2. The GISP2 core has shown the glacial accumulation rate to be approximately one-third that of the Holocene (24). For this accumulation rate contrast, two analyses of Dye 3 temperature (16, 44) indicate an approximately  $14^{\circ}\text{C}$  deglacial temperature change.

43. For summary, see J. T. Houghton, G. J. Jenkins, J. J. Ephraums, Eds., *Climate Change: The IPCC Scientific Assessment* (Cambridge Univ. Press, Cambridge, 1990).

44. J. Firestone, *J. Glaciol.* **41**, 39 (1995).

45. Our filter is the resolution kernel of Backus-Gilbert inversion; W. Menke, *Geophysical Data Analysis:*

*Discrete Inverse Theory* (Academic Press, San Diego, revised ed., 1989), pp. 71–72.

46. N. S. Gundestrup, D. Dahl-Jensen, S. J. Johnsen, A. Rossi, *Cold Reg. Sci. Tech.* **21**, 399 (1993); analyses pending (D. Dahl-Jensen and S. Johnsen, in preparation).

47. For the “no north-south spreading,” we assumed that the ice flow is two-dimensional (east-west and vertical). The uncorrected accumulation rate history has not been corrected for thickness changes of the ice sheet. For “no fabric evolution,” there is no enhancement of ice softness for ice deposited during glacial times.

48. This work was supported by the NSF (some material is based on work supported by a NSF Graduate Research Fellowship) and the U.S. Geological Survey. We thank the GISP2 Science Management Office, the 109th Air National Guard, the Polar Ice Coring Office, and GISP2 participants.

31 May 1995; accepted 18 August 1995

## Superplasticity in Earth's Lower Mantle: Evidence from Seismic Anisotropy and Rock Physics

Shun-ichiro Karato,\* Shuqing Zhang, Hans-Rudolf Wenk

In contrast to the upper mantle, the lower mantle of the Earth is elastically nearly isotropic, although its dominant constituent mineral [(Mg,Fe)SiO<sub>3</sub> perovskite] is highly anisotropic. On the basis of high-temperature experiments on fabric development in an analog CaTiO<sub>3</sub> perovskite and the elastic constants of MgSiO<sub>3</sub> perovskite, the seismic anisotropy was calculated for the lower mantle. The results show that absence of anisotropy is strong evidence for deformation by superplasticity. In this case, no significant transient creep is expected in the lower mantle and the viscosity of the lower mantle is sensitive to grain size; hence, a reduction in grain size will result in rheological weakening.

Rheological properties have an important influence on the nature of flow in the deep interior of the Earth, but both laboratory and theoretical studies of deep mantle rheology have significant limitations. Quantitative measurements of the strength of materials under high pressures and temperatures are difficult, and no rheological measurements have been performed under lower mantle conditions. Neither the rheological constitutive relation (that is, the dependence of viscosity on stress or grain size or both) nor the absolute values of viscosity of the lower mantle are well constrained (1). The rheology of the Earth's deep interior can be inferred from laboratory data only after a large extrapolation in time scales, which introduces a significant amount of uncertainty. Similarly, theoretical estimates of rheological properties of the Earth's deep interior from time-dependent deformation are difficult to make because of (i) the poor sensitivity of the data to rheo-

logical properties of the deep portions of the Earth (2), (ii) the uncertainties in some key input parameters such as the melting history of ice sheets (3) in the analysis of the postglacial rebound, or (iii) the density-to-velocity conversion factor (4) in the analysis of the geoid.

One strategy to get around these difficulties is to combine seismological observations of anisotropy and laboratory studies of deformation-induced lattice preferred orientation [for example (5)]. The anisotropic structure of deformed materials depends on deformation mechanisms (and deformation geometry) [for a review, see (6)], and anisotropic structures can be observed seismologically as far down as the center (that is, inner core) of the Earth (7). Plastic deformation by diffusion or superplastic creep will result in an isotropic structure, whereas deformation by dislocation creep or twinning results in an anisotropic structure. Thus, although this approach will not provide direct estimates of the absolute values of viscosities, it provides information as to the rheological constitutive relation (stress or grain-size dependence of viscosity) and hence indirectly indicates rheological discontinuities or weakening associated with

grain-size reduction (5, 8).

Here we apply this strategy to the lower mantle. One of the most striking observations of the lower mantle is the absence of significant seismic anisotropy (9) even though the dominant mineral in the lower mantle, orthorhombic (Mg,Fe)SiO<sub>3</sub> perovskite, has significant elastic anisotropy (10, 11). The absence of observed anisotropy in the lower mantle could be attributed to (i) chaotic convection; (ii) limited plastic deformation; (iii) the anisotropic structure in the lower mantle which happens to be such that, for seismic waves traveling nearly vertically [such as those used in seismological studies (9)], the amount of shear wave splitting is small (12); or (iv) the fact that the deformation does not result in an anisotropic structure. The first hypothesis means that the lower mantle materials could have anisotropic structure (possibly due to deformation by dislocation creep), but the scale of coherent deformation is much smaller than the length of typical seismic wave paths (for ScS or SKS) so that, on average, no appreciable anisotropy would be detected. This hypothesis is unlikely because seismic tomography indicates that the lower mantle structure is dominated by long wave length features (13), and a high viscosity of the lower mantle will make chaotic convection difficult to achieve (14). The second hypothesis is also untenable because seismic tomography indicates the presence of downgoing and upwelling currents in the lower mantle (15), and the Rayleigh number for the lower mantle is likely to exceed the critical value [see, for example, (1)]. Discrimination of the last two alternatives requires an investigation of the relation between the nature of deformation and seismic anisotropy in lower mantle materials.

The most direct data on this subject must ultimately come from high-pressure, high-temperature deformation experiments performed on polycrystalline (Mg,Fe)SiO<sub>3</sub>

S.-i. Karato and S. Zhang, Department of Geology and Geophysics, University of Minnesota, Minneapolis, MN 55455, USA.

H.-R. Wenk, Department of Geology and Geophysics, University of California, Berkeley, CA 94720, USA.

\*To whom correspondence should be addressed.